Title	Relationship between Surface Potential Difference and Galvanic Corrosion of Magnesium Alloy Using SKPFM
Author(s)	Takei, Rei; Imai, Hisashi; Umeda, Junko et al.
Citation	Transactions of JWRI. 2010, 39(1), p. 75-80
Version Type	VoR
URL	https://doi.org/10.18910/10157
rights	
Note	

Relationship between Surface Potential Difference and Galvanic Corrosion of Magnesium Alloy Using SKPFM [†]

TAKEI Rei*, IMAI Hisashi**, UMEDA Junko*** and KONDOH Katsuyoshi****

Abstract

Magnesium (Mg) which has the lowest negative standard electrode potential among industrial metals, results in the easy corrosion phenomenon in contact with other metals due to the formation of a galvanic cell at the interface. The traditional methods to evaluate corrosion resistance such as saltwater immersion test, salt spray test, and electrochemical corrosion test provide the macroscopic corrosion phenomenon, but not microscopic information at the local interface. It is important and necessary to clarify galvanic corrosion mechanism at the interface between α-Mg matrix and metallic dispersoids of Mg alloys. In the present study, the surface potential difference (ΔV_{SPD}) at the interface between dispersoids and α-Mg of Mg-Fe cast material and AZ91D alloy was measured by using Scanning Kelvin Probe Force Microscope (SKPFM). Surface potentials of pure metals measured by SKPFM showed good correlation with standard electrode potentials (SEP), and ΔV_{SPD} values also corresponded with the theoretical values of the difference in SEP. Salt water immersion test of AZ91D alloy was conducted to clarify the relationship between ΔV_{SPD} measurements and corrosion resistance. Changes in topographic maps around the intermetallic dispersoids were investigated by using AFM before and after corrosion tests, and showed that corroded phases corresponded to the anodic phases indicated by surface potential.

KEY WORDS: (Magnesium) (Galvanic Corrosion) (Surface Potential) (SKPFM)

1. Introduction

Magnesium (Mg) alloys, having high specific strength and stiffness due to their low density of 1.7 g/cm³, are applied to industrial components such as transport products and mobile electronic devices. They are expected to improve fuel efficiency and to reduce CO_2 gas emission in the automobile[1-3]. However, one of the disadvantages of the conventional Mg alloys is poor corrosion resistance[1-3], and some protecting surface coating is necessary in the use of Mg alloys as structural components. Pure Mg has a lower standard electrode potential (SEP) of -2.363V compared with other traditional metals such as Fe, Ni, Cu. This means that Mg easily becomes the anodic side of a galvanic cell when some electric potential occurs by contact with other metals[4]. The greater the difference of SEP, the more corrosion proceeds[5,6]. Therefore, the galvanic corrosion behavior contacting with other pure metals can be approximately evaluated by considering their values

of SEP. On the other hand, the galvanic corrosion phenomenon of Mg alloys has been investigated by salt water immersion test, salt spray test and electrochemical corrosion test[7-10]. They are suitable for evaluation of macroscopic behavior of corrosion phenomenon of Mg alloys. In other words, it is difficult for these analytical methods to quantitatively evaluate the local galvanic corrosion at the interface between intermetallic dispersoids and α-Mg matrix. The present study focused on the relationship between surface potential difference (ΔV_{SPD}) at the interface and corrosion phenomenon, and indicated a possibility of using ΔV_{SPD} measured by Scanning Kelvin Probe Force Microscope (SKPFM) for quantitative evaluation of the local galvanic corrosion phenomenon. First of all, the relationship between ΔV_{SPD} and difference of SEP was investigated experimentally and theoretically by using SKPFM analysis of pure metals (Mg, Al, Cu, Fe, Ni etc.) to evaluate the reliability of the measurement. The conventional cast Mg alloy, AZ91D containing $Mg_{17}Al_{12}$ (β phase) and Al_6Mn

intermetallic compounds were used to investigate ΔV_{SPD} values of each compound and galvanic corrosion phenomena at the interface. Furthermore, a salt water immersion test was employed for corrosion phenomenon evaluation, and the results were quantitatively compared with ΔV_{SPD} measurements by SKPFM. After the corrosion test, a topographic map analyzed by AFM attached to SKPFM equipment provided information for the identification of corroded phase.

2. Experimental Procedure

2.1 Principal of SKPFM for surface potential evaluation

The surface potential measured by Scanning Kelvin Probe Force Microscope (SKPFM, Shimadzu SPM-9600) is the contact potential difference V_{CPD} between the sample specimen and the cantilever probe coated with PtIr5. V_{CPD} value is obtained by subtracting the work function of the sample metal ϕ_{sample} from that of PtIr5 ϕ_{PtIr5} and then dividing by elementary electric charge, as shown in the following equation:

$$V_{CPD}= (\phi_{PtIr5} - \phi_{sample}) / e \tag{1}$$

The variation tendency of this surface potential is different from that of SEP. The work function is the minimum energy needed to remove an electron from a solid into vacuum. It can be represented by using the equation[11,12] below, where χ represents the Pauling's electronegativity[13].

$$\phi = 2.27\chi + 0.34 \tag{2}$$

The relationship between the work function obtained using the above equation and SEP[14] is shown in **Fig. 1**. This correlation indicates that the work function of low SEP metals generally has small values. Therefore, the surface potential (V_{CPD}) of low SEP metals (i.e. Mg and Al) is higher, because the smaller work function results in higher V_{CPD} according to the above equation (1). The V_{SPD} value between Mg and other metals is calculated as shown below.

$$\Delta V_{SPD} = V_{Mg} - V_{Metal}$$
$$= (\phi_{PtIr5} - \phi_{Mg}) / e - (\phi_{PtIr5} - \phi_{Metal}) / e$$
$$= (\phi_{Metal} - \phi_{Mg}) / e \tag{3}$$

In addition, the difference of SEP is also defined using the following equation, where V_{Metal} and V_{Mg} are SEP of contacted metal and Mg, respectively.
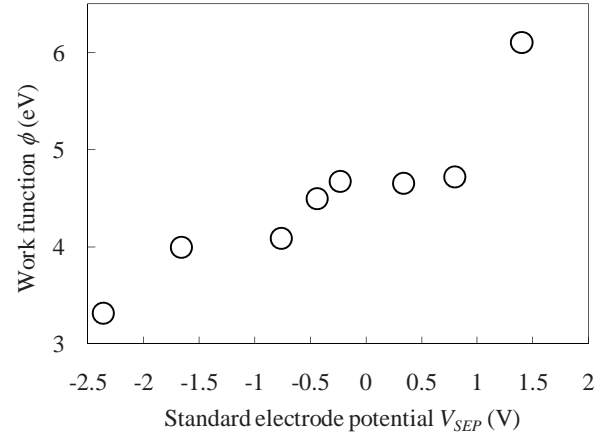
$$\Delta V_{SEP}=V_{Metal} - V_{Mg} \tag{4}$$

Fig. 1   Relationship between standard electrode potential and work function.

The values of theoretical ΔV_{SPD} and ΔV_{SEP} are shown in **Table 1** using both eq. (3) and eq. (4). ΔV_{SPD} is approximately proportional to ΔV_{SEP}. It is concluded that the galvanic corrosion of Mg alloy at the interface between α-Mg and intermetallic dispersoids can be quantitatively evaluated using ΔV_{SPD} measured by SKPFM and the effect of the local ΔV_{SPD} on the galvanic corrosion behavior is investigated in the present study.

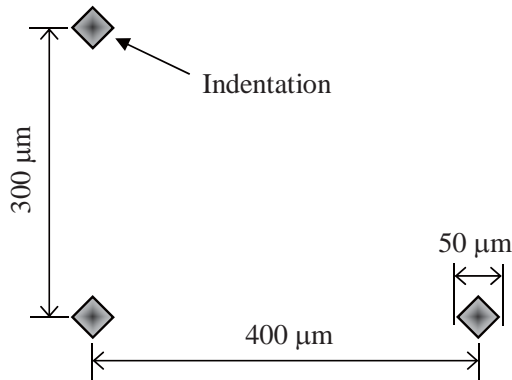### 2.2 Materials and evaluation of galvanic corrosion

For evaluation of the corrosion behavior of materials by ΔV_{SPD} measured in SKPFM system, the surface potential was first investigated by using pure metals such as magnesium, aluminum, zinc, iron, nickel, copper, silver and gold, and ΔV_{SPD} values were calculated from measurements (V_{Metal}) using the above eq. (3). These experimental results of ΔV_{SPD} were compared to the theoretical values shown in **Table 1**. To investigate the surface potential difference (ΔV_{SPD}) at the interface of Mg alloys by SKPFM system, two materials were prepared as follows; one was pure cast Mg including Fe particle dispersoids and another was the conventional Mg alloy, AZ91D cast material (Al; 9.1, Zn; 0.88. Mn; 0.17, Si; 0.01, Fe; 0.003, Cu<0.002, Ni<0.002 / mass%, Mg; Bal). For the fabrication of the former material, pure Fe fine powders, having a mean particle size of about 2mm, were casted into molten pure Mg at 1073K under an argon gas atmosphere in carbon crucible. The reason why Fe particles were selected as second phases of pure

Table 1   Values of ΔV_{SEP} and theoretical ΔV_{SPD}.

Contacted metal	Al	Zn	Fe	Ni	Cu	Ag	Au
ΔV_{SEP} (V)	0.7	1.6	1.92	2.13	2.7	3.16	3.76
ΔV_{SPD} (V)	0.681	0.7718	1.1804	1.362	1.3393	1.4074	2.7921

Table 2 Conditions of salt water immersion test used in this study.

Concentration (mass%)	5
Solution temperature (K)	303
Testing time (h)	18
Initial pH	6.24

Fig. 2 Two dimensional coordinate on specimen surface by indentations.

Mg was because in general Fe impurities contained in Mg alloys accelerated the galvanic corrosion phenomenon[3]. Accordingly, ΔV_{SPD} measurement between pure Fe and Mg could be used as a useful reference point to decide the negative impact of the other metallic dispersoids of Mg alloys on the corrosion behavior. In the experiment, the surface polishing of each specimen was conducted using water-proof abrasive paper up to #4000 in tap water. Then, the mirror finish treatment was delivered to the surface by buffing using diamond paste. In the case of AZ91D cast alloy, the ΔV_{SPD} values between α-Mg and $Mg_{17}Al_{12}$ or Al-Mn compounds were measured at ambient temperature.

On the other hand, the traditional salt water immersion test was applied to these Mg specimens to evaluate corrosion behavior. The test conditions were shown in **Table 2**. SEM observation and AFM topographic mapping methods were used to analyze surface changes at the same position of the specimens before and after the corrosion tests. When pure metals or the interfacial phase of Mg and Fe are scanned, the scanning point can be identified by using an optical microscope equipped with this SKPFM. The magnifications of this optical microscope are from 84 to 525 times. However, microstructural identification of very fine dispersoids of Mg alloys is extremely difficult by this optical microscope. The present study suggests a unique method to identify fine dispersoids by using indentations of Vickers hardness tester. The X-Y 2 dimensional coordinate is formed on the mirror polished surface of the specimen by the identification schematically illustrated in **Fig. 2**, and the relative position of the dispersoids can be fixed in the coordinate. The specific process for identifying them is as follows; first of all, one indentation is produced at an arbitrary position. Then, second and third indentations are produced at 400μm apart from the first indentation in the horizontal axis direction and at 300μm apart from the first indentation in the vertical axis direction, as shown in Fig. 2. After that, the relative position of each dispersoid against the three indentations is captured on the scanning electron microscope (SEM, JEOL JSM-6500F) image. That dispersoid is identified by using both energy-dispersive X-ray spectroscopy (EDS, JEOL JED-2300) analysis and X-ray diffraction (XRD, Shimadzu XRD-6100) analysis. After identifying the position of the dispersoid by the three indentations in the coordinate, the dispersoid can be identified by the optical microscope equipped with SKPFM. The cantilever is then moved to this point, and scanning the square area at that point starts. The square area includes dispersoid and α-Mg, so that the interfacial ΔV_{SPD} between dispersoid and α-Mg can be measured in this system.

3. Results and discussion

Table 3 indicates the measured surface potential of pure metal specimens by SKPFM system, and the correlation between ΔV_{SPD} experimental measurements and ΔV_{SEP} theoretical values is shown in **Fig. 3**. This result shows a good correspondence to the theoretical values shown in **Table 1**. This means that the SKPFM system has a high reliability in measuring the surface
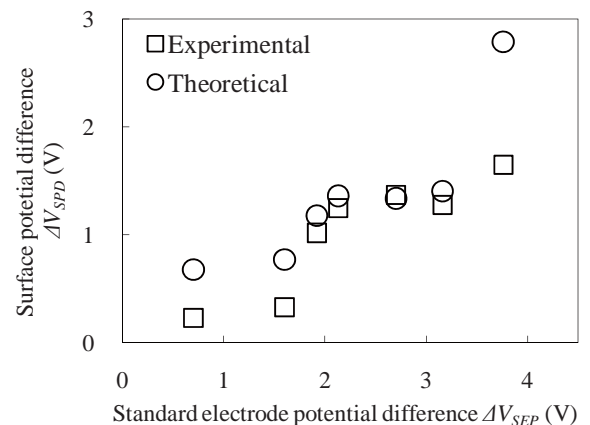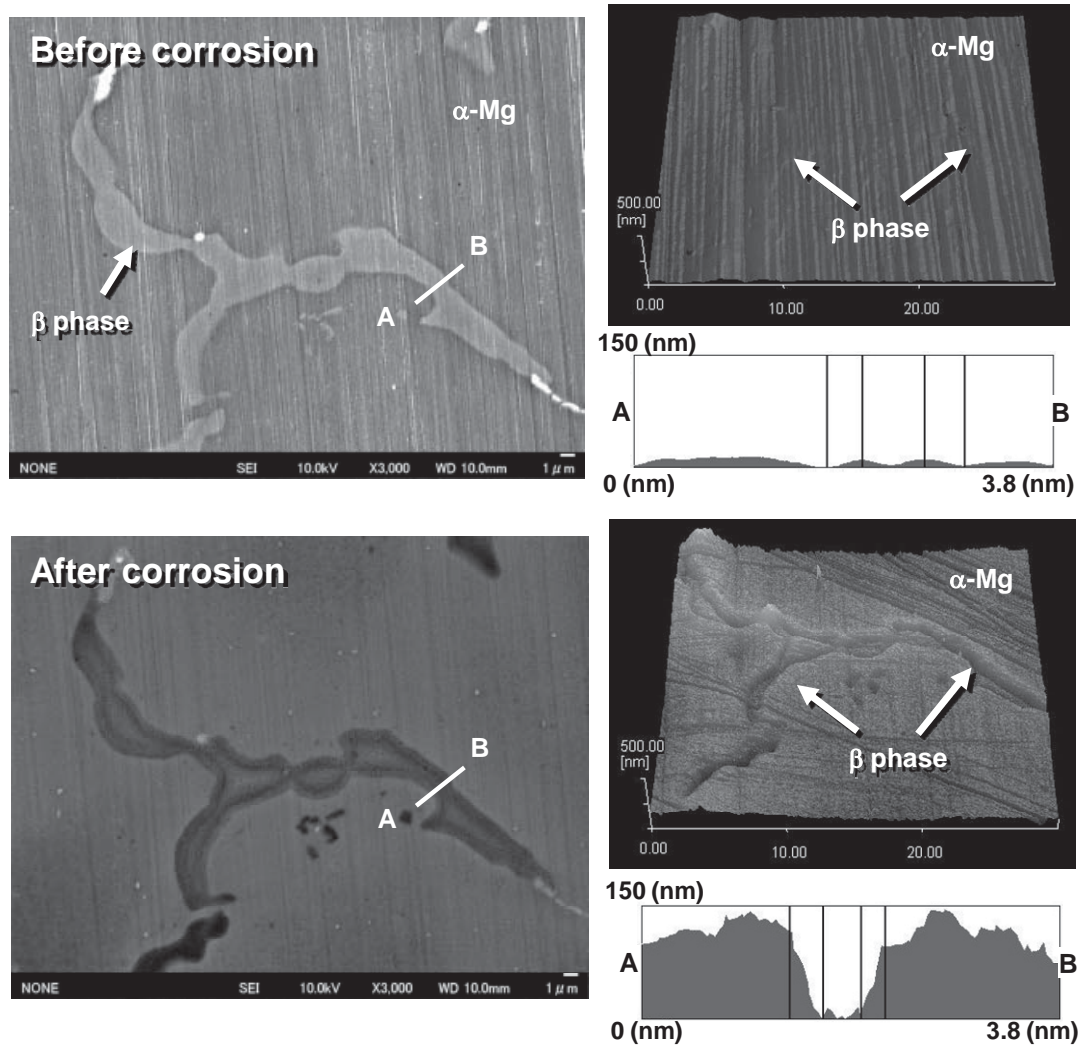

Fig. 3 Relationship between difference of SEP and ΔV_{SPD}.

Table 3 Surface potential measurements of pure metal specimens.

Pure Metal	Mg	Al	Zn	Fe	Ni	Cu	Ag	Au
Surface Potential (V)	1.32	1.04	1.00	0.30	0.07	-0.05	0.02	-0.33

Table 4 Surface potential difference at interface of each Mg material.

Measurement point	Mg - Fe	α-Mg - α-Mg	α-Mg - Mg$_{17}$Al$_{12}$	α-Mg - Al-Mn
ΔV_{SPD} (V)	-0.84 ± 0.057	0.022 ± 0.011	0.05 ± 0.011	-0.48 ± 0.024

Fig. 4(a) SEM observation of β phase before and after salt water immersion test and topography around β phase and cross section view of height at A-B line.

potential difference of materials and could provide ΔV_{SPD} measurements at the interface of Mg alloys.

The ΔV_{SPD} values at the interface between the dispersoid and α-Mg matrix of Mg materials measured by SKPFM are shown in **Table 4**, where the dispersoids are Mg$_{17}$Al$_{12}$, Al-Mn, and Fe. The measurement is expressed in the form of average added standard deviation. Negative sign indicates that the surface

potential of each dispersoid is lower than that of α-Mg. The ΔV_{SPD} between Mg$_{17}$Al$_{12}$ and α-Mg is twice as large as that between two points of α-Mg, and is considerably smaller than that of Mg−Fe and α-Mg−Al-Mn. Furthermore, the surface potential of Mg$_{17}$Al$_{12}$ is higher than that of α-Mg. This means Mg$_{17}$Al$_{12}$ phase becomes anodic in galvanic corrosion phenomenon. On the other hand, the ΔV_{SPD} between Al-Mn and α-Mg is much
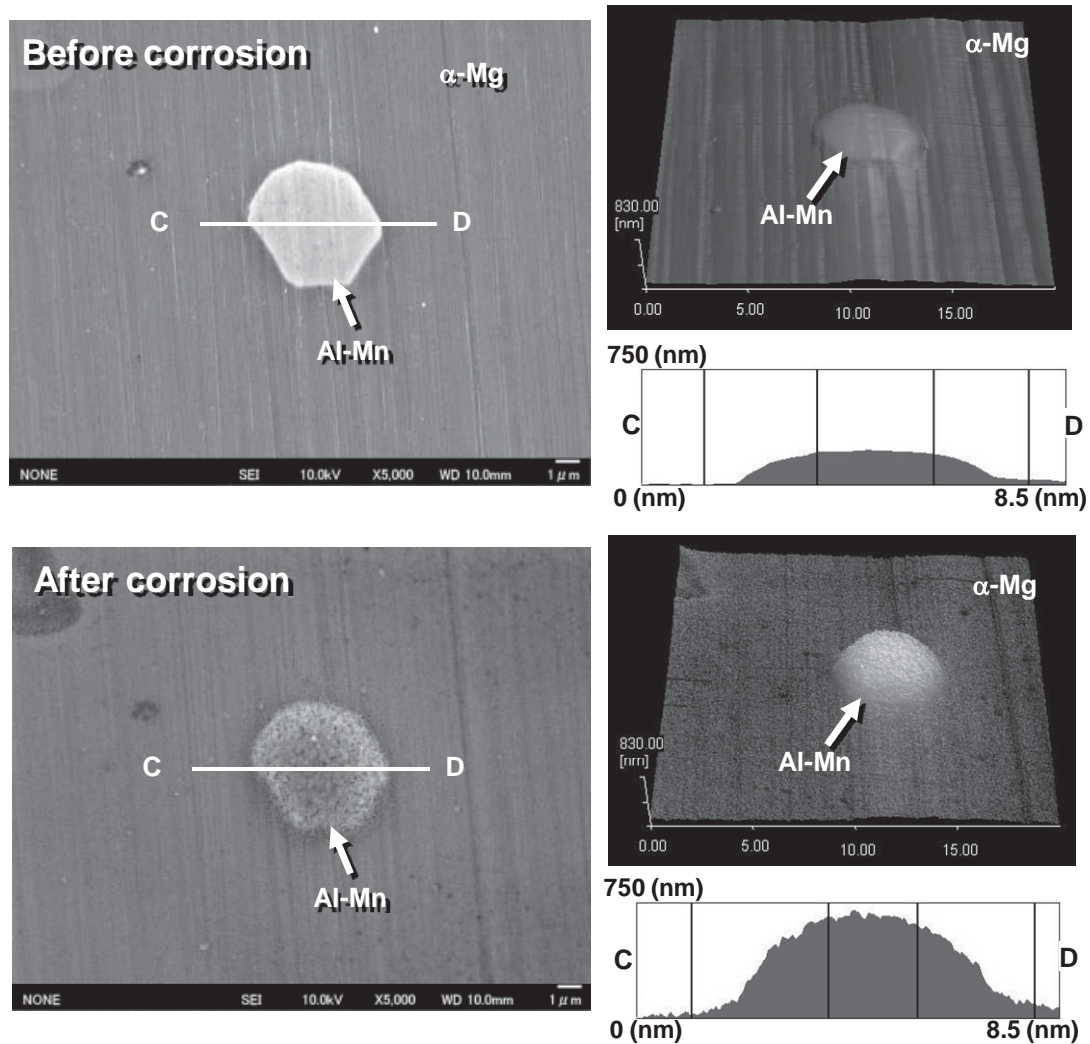
Fig. 4(b) SEM observation of Al-Mn phase before and after salt water immersion test and topography around dispersoid and cross section view of height at C-D line.

Table 5 Changes in height of dispersoids before and after salt water immersion test.

		Height (nm)		Difference (nm)
		Before corrosion	After corrosion	
α-Mg – β phase		5 – 20	90	102
α-Mg – Al-Mn	Right	158	517	359
	Left	184	435	251

larger than that of $Mg_{17}Al_{12}$, and about a half of the value of Mg–Fe. The surface potential of Al-Mn is lower than that of α-Mg, with the result that Al-Mn compound becomes cathodic. **Figure 4** indicates SEM observation results on microstructural changes around $Mg_{17}Al_{12}$ and Al-Mn compounds and topographic mapping results at these dispersoids by AFM before and after the salt water immersion test. In particular, the cross-section view of

height measured at A-B and C-D lines of AZ91D cast alloy. Both specimens after corrosion test indicate surface damages due to galvanic corrosion at each interface. Topographic maps before and after corrosion test provide changes in the height difference of specimens shown in **Table 5**. $Mg_{17}Al_{12}$ is earlier corroded at the interface than α-Mg matrix, and the height change is about 100nm by galvanic corrosion. On

the other hand, a rise is obviously observed in the Al-Mn compound, and its height change is relatively large compared to the specimen surface before corrosion test. This is due to corrosion products deposited on Al-Mn compounds. These results indicate that corroded phases correspond to the anodic materials indicated by surface potential and the potential measurements by SKPFM have good correlation with corrosion phenomenon theoretically and experimentally.

4. Conclusion

The SKPFM system has been established to quantitatively evaluate corrosion resistance at the interface between dispersoids and α-Mg by using ΔV_{SPD} measurements. The correlation between ΔV_{SPD} and galvanic corrosion behavior was investigated by SKPFM and SEM observation. The results obtained in the present study were summarized as follows:

(1) Surface potential of low SEP metal was generally high. ΔV_{SPD} also had positive correlation with ΔV_{SEP}, theoretically and experimentally. Therefore, galvanic corrosion can be evaluated using ΔV_{SPD} at the interface between dispersoids and α-Mg.

(2) The ΔV_{SPD} between $Mg_{17}Al_{12}$ and α-Mg was approximately twice as large as the ΔV_{SPD} within α-Mg, and the surface potential of $Mg_{17}Al_{12}$ was higher than that of α-Mg by 0.05V. On the other hand, ΔV_{SPD} between Al-Mn and α-Mg was much larger than that of $Mg_{17}Al_{12}$ and was two-thirds as large as that of Mg-Fe. The surface potential of Al-Mn was lower than that of α-Mg by 0.48V, and so galvanic corrosion at the interface of Al-Mn occurs more severely than that of $Mg_{17}Al_{12}$.

(3) Salt water immersion tests conducted for comparison between ΔV_{SPD} and early corrosion phenomenon revealed anodic reaction of $Mg_{17}Al_{12}$ and cathodic reaction of Al-Mn at each interface. These phases corresponded to the phase indicated by surface potential at the interface. Therefore, this method using ΔV_{SPD} measured by SKPFM is very suitable to evaluate galvanic corrosion locally.

Reference

1) D.F. Miner, J.B. Seastone, Handbook of Engineering Materials, Wiley, New York, 1955.
2) M.M. Avedesian, H. Baker, Magnesium and Magnesium Alloys, ASM International, OH, 1999.
3) J. R. Davis, Metals Handbook 2nd Edition, ASM International, OH, 1998, pp.570-574.
4) G. Song, B. Johannesson, S. Hapugoda, D. StJohn, Galvanic corrosion of magnesium alloy AZ91D in contact with an aluminium alloy, steel and zinc, Corros. Sci. 46 (2004) 955.
5) C. Carraro, R. Maboudian, L. Magagnin, Surface Science Reports, 62 (2007) 499.
6) S. Bilouk et al., Microelectronic Engineering, 86 (2009) 2038-2044.
7) G. Ballerini, U. Bardi, R. Bignucolo, G. Ceraolo, Corrosion Science, 47 (2005) 2173–2184.
8) J.W. Chang, P.H. Fu, X.W. Guo, L.M. Peng, W.J. Ding, Corrosion Science 49 (2007) 2612–2627.
9) M.C. Zhao, P. Schmutz, S. Brunner, M. Liu, G. Song, A. Atrens, Corrosion Science 51 (2009) 1277–1292.
10) S. Izumi, M. Yamasaki, Y. Kawamura, Corrosion Science 51 (2009) 395–402.
11) W. Gordy, W. J. O. Thomas, J. Chem. Phys., 24 (1956) 439.
12) J.K. Schaeffer et al., Microelectronic Engineering, 84 (2007) 2196-2200.
13) A.L. Allred, Electronegativity values from thermo-chemical data, J. Inorg. Nucl. Chem., 17 (1961) 219.
14) P.W. Atkins, Physical Chemistry Sixth Edition, Oxford University Press, Oxford, (1998) 934-936.